Supplementary Information

Spontaneous Formation of Gold Nanoparticles Triggered by Hydrophobic Interfaces

Yuina Yagi[1], Takahiro Kozawa[2,], Kanako Yoshida[2], Akihiro Uehara[3], Minoru Osada[4] and Hiroya Abe[2,*]*

1. Graduate School of Engineering, The University of Osaka, Osaka 565-0871, Japan
2. Joining and Welding Research Institute, The University of Osaka, Osaka 567-0047, Japan
3. Institute for Radiological Science, National Institutes for Quantum Science and Technology, Chiba 263-8555, Japan
4. Department of Materials Chemistry & Institute of Materials and Systems for Sustainability (IMaSS), Nagoya University, Aichi 464-8601, Japan

*Corresponding author.
Takahiro Kozawa, E-mail: kozawa.takahiro.jwri@osaka-u.ac.jp
Hiroya Abe, E-mail: abe.hiroya.jwri@osaka-u.ac.jp

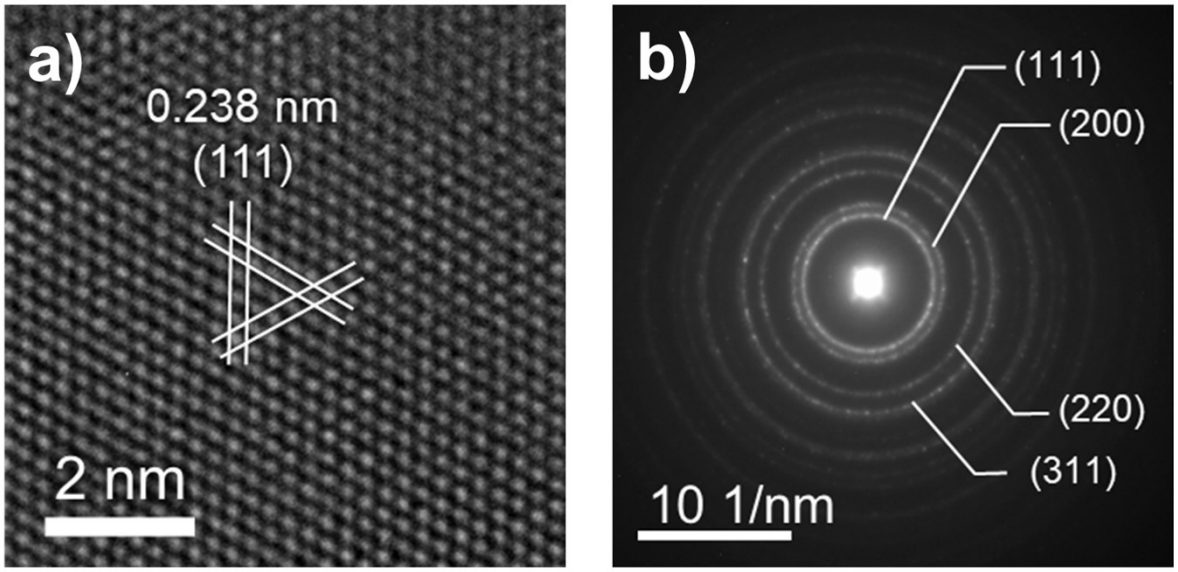

Figure S1. Structural characterization of the synthesized AuNPs. (a) High-resolution TEM image showing a lattice spacing of 0.238 nm, corresponding to the (111) plane of fcc Au. (b) Selected area electron diffraction (SAED) pattern confirming the fcc crystal structure of the developed AuNPs.

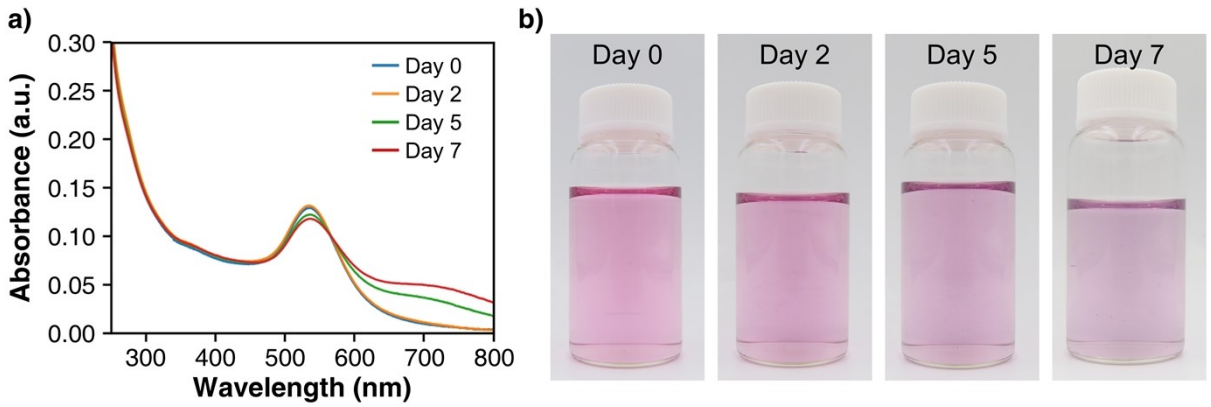

Figure S2. Colloidal stability of AuNPs synthesized under standard conditions (pH 12, 80 °C, 20 h, PFA vessel). (a) UV–vis spectra and (b) photographs up to 7 days.

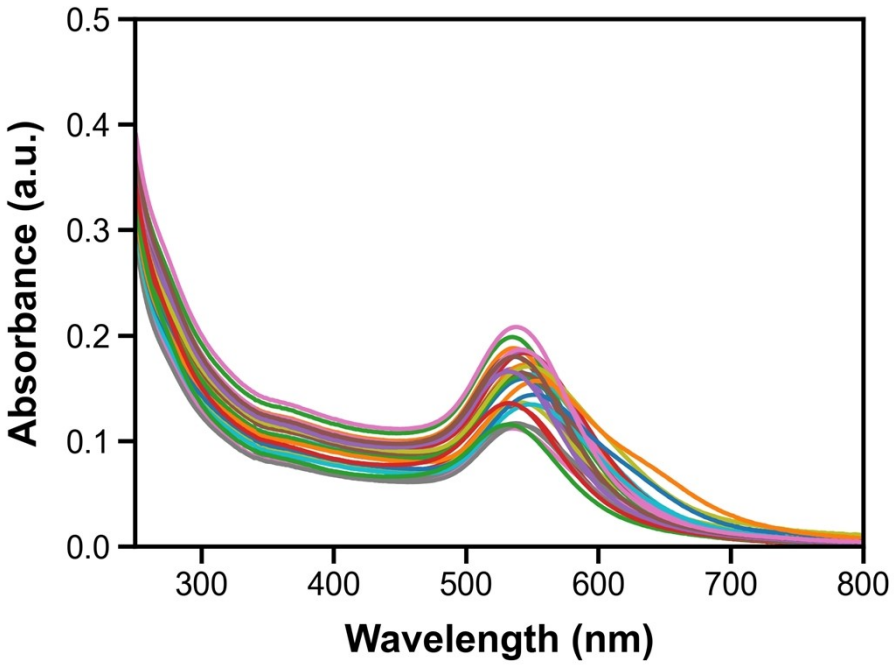

Figure S3. Reproducibility of AuNP synthesis under standard conditions (pH 12, 80 °C, 20 h, PFA vessel). UV–vis measurements were performed on 27 independently synthesized samples.

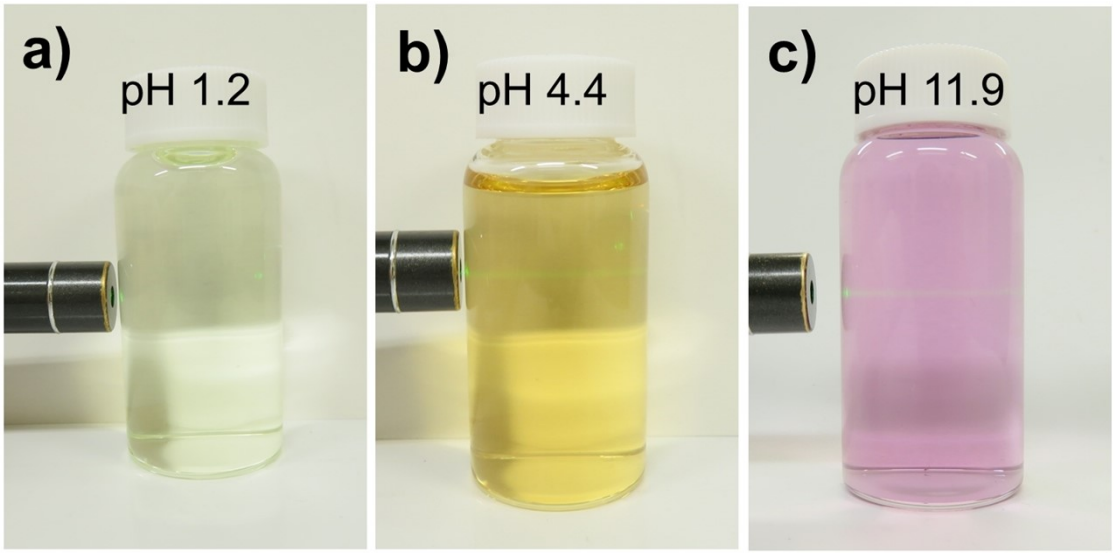

Figure S4. Photographs of the Tyndall effect under different pH conditions. (a) Strongly acidic condition (pH ≈ 1): the solution remained pale yellow after heating, and no visible Tyndall effect was observed, indicating the absence of nanoparticle formation. (b) Weakly acidic conditions (pH 3–5): the solution became more intensely yellow after heating, and a clear Tyndall effect was observed, suggesting the formation of dispersed particulate species. (c) Basic conditions (pH > 10): the solution turned red after heating, and a distinct Tyndall effect was observed, indicating the formation of colloidal AuNPs.

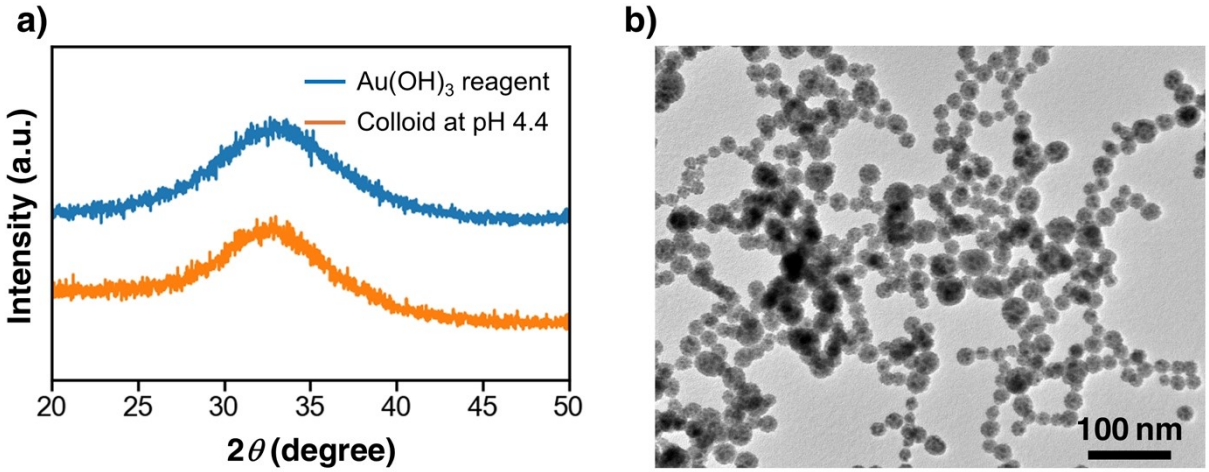

Figure S5. Characterization of the precipitate obtained under weakly acidic conditions (pH 4.4). (a) XRD pattern and (b) TEM image of the precipitate. The diffraction pattern is consistent with that of the $Au(OH)_3$ reagent, indicating that $Au(OH)_3$ is the predominant product under these conditions. The precipitated $Au(OH)_3$ particles were spherical with an average diameter of approximately 22 nm.

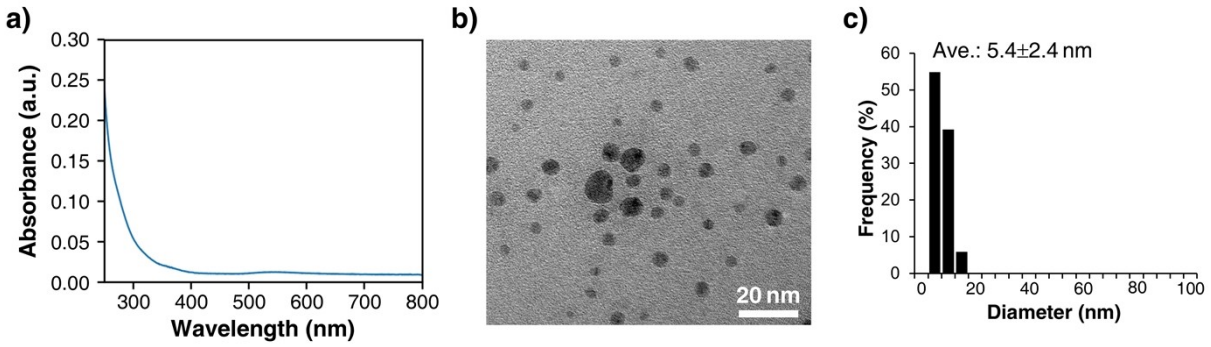

Figure S6. (a) UV–vis spectrum, (b) TEM image, and (c) particle size distribution of the product obtained from the initial $HAuCl_4$ concentration of 1 mM at pH 12.7, 80 °C, for 20 h in a PFA vessel.

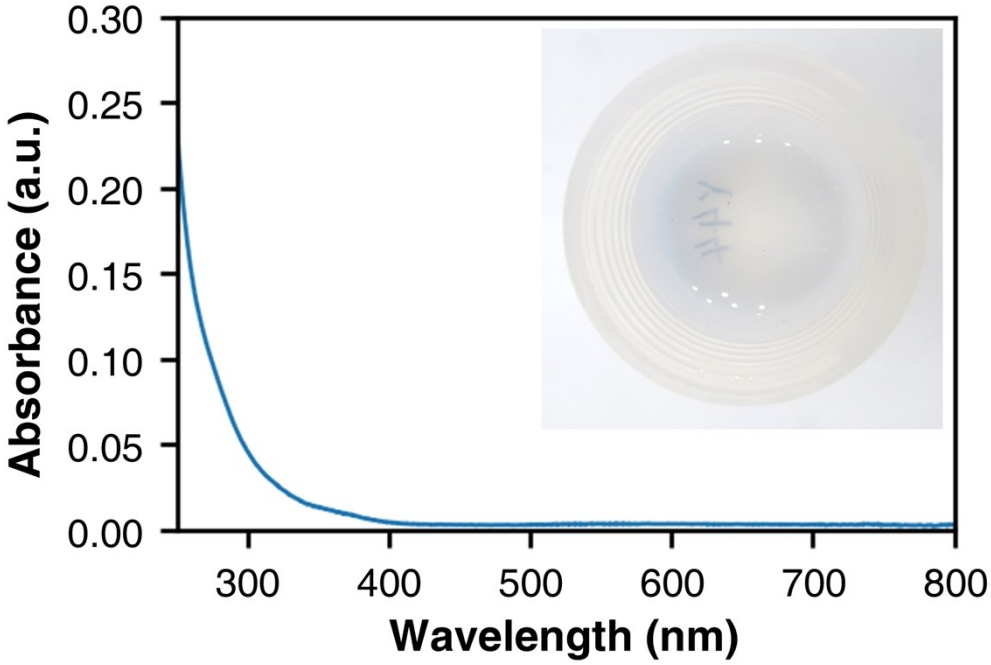

Figure S7. UV–vis spectrum and photograph of the product obtained at pH 14, 80 °C, for 20 h in a PFA vessel.

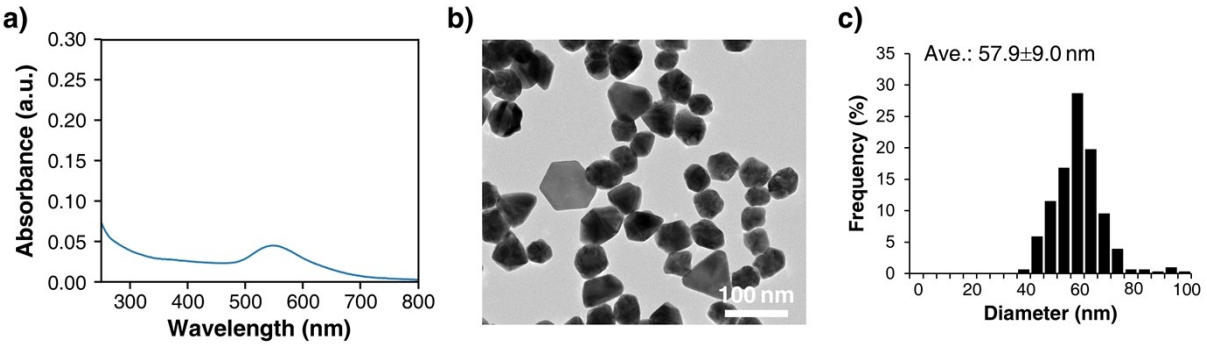

Figure S8. (a) UV–vis spectrum, (b) TEM image, and (c) particle size distribution of the product obtained from the initial $HAuCl_4$ concentration of 0.2 mM at pH 12.0, 80 °C, for 20 h in a PFA vessel.

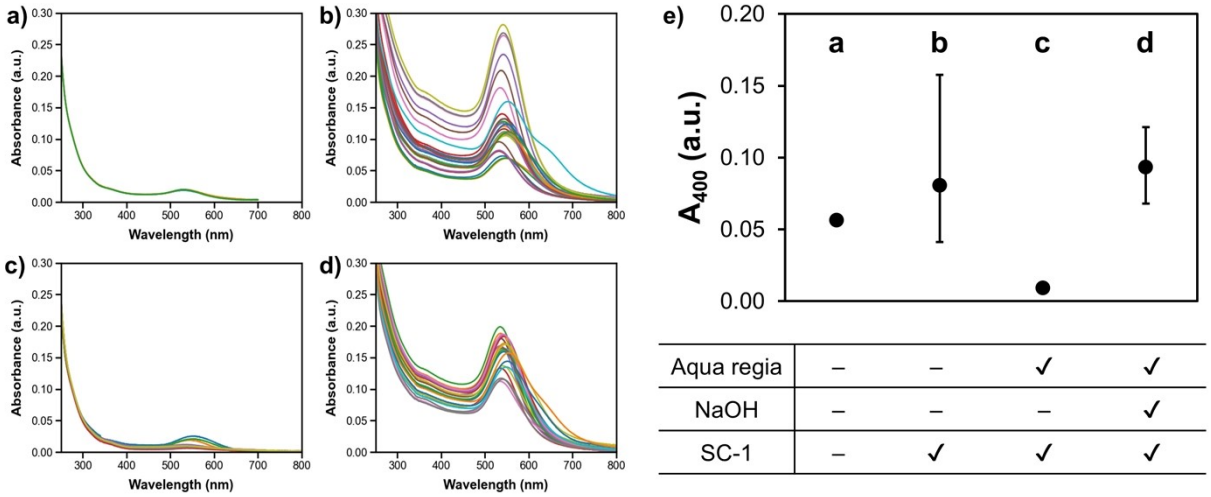

Figure S9. Influence of vessel cleaning protocols on AuNP formation in hydrophobic PFA vessels. (a–d) UV–vis spectra of reaction solutions obtained under different cleaning protocols: (a) no cleaning; (b) SC-1 cleaning only; (c) aqua regia followed by SC-1 cleaning; (d) three-step cleaning (aqua regia, heated NaOH rinse, and SC-1). (e) Comparison of absorbance at 400 nm, indicating synthesis yield, across conditions (a–d), showing the minimum, maximum, and average values for each condition.

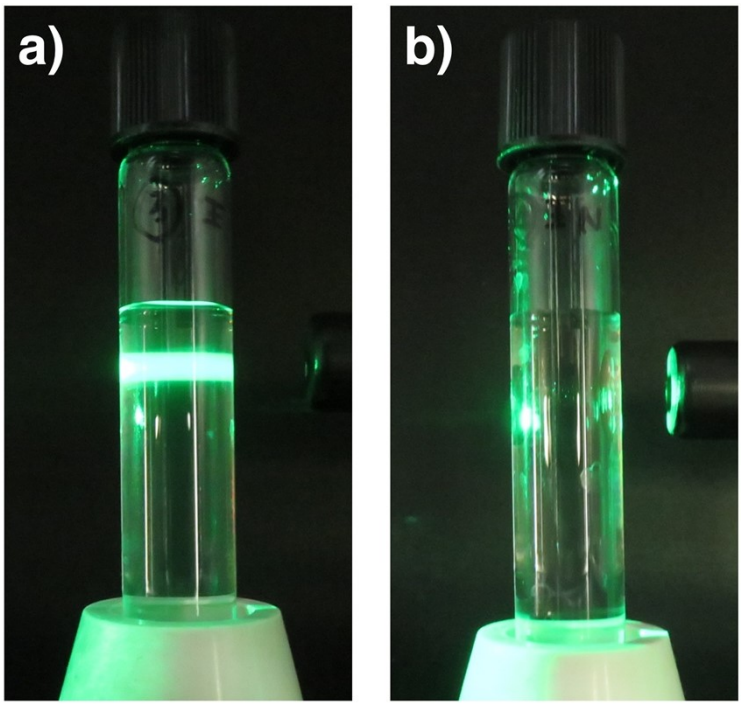

Figure S10. Tyndall scattering images of solutions after adding $AgNO_3$ aqueous solution to water shaken in PFA vessels cleaned by (a) aqua regia only, showing visible Tyndall scattering indicative of AgCl formation, and (b) aqua regia followed by NaOH rinsing, showing no Tyndall scattering.

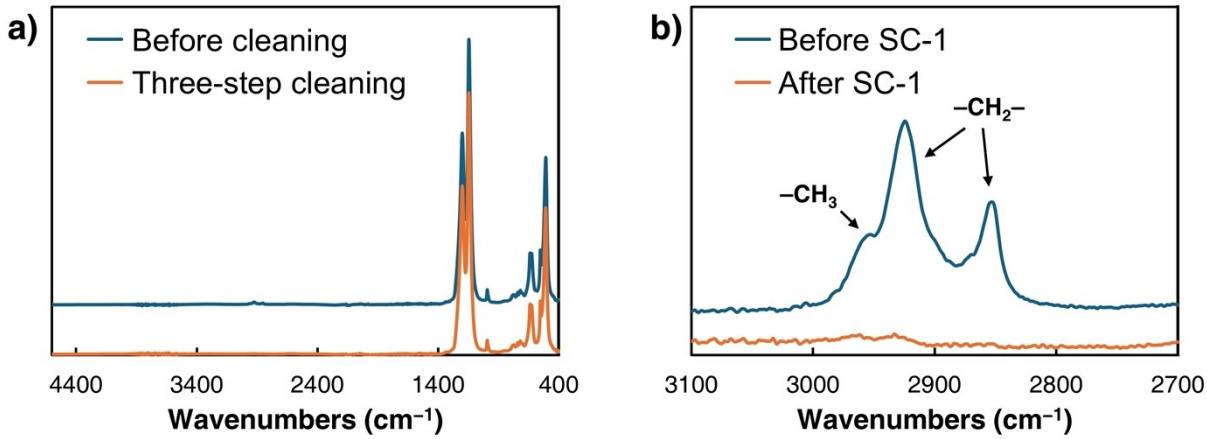

Figure S11. FTIR spectra of PFA substrates: (a) before and after the three-step cleaning protocol, and (b) an expanded view of the 2700–3100 cm^{-1} region after SC-1 cleaning.

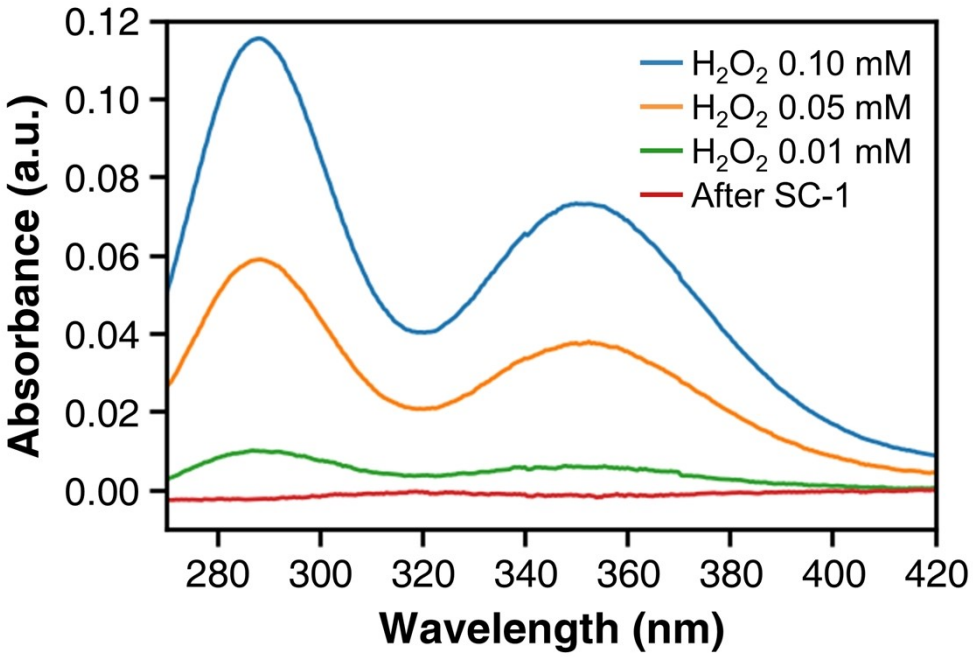

Figure S12. UV–vis spectra obtained after adding KI solution (200 mM) to aqueous H_2O_2 solutions (0.01–0.1 mM) and post-wash water from a PFA vessel cleaned by the SC-1 method. Triiodide (I_3^-), formed by oxidation of iodide with H_2O_2, exhibits characteristic absorption bands near 290 nm and 350 nm.

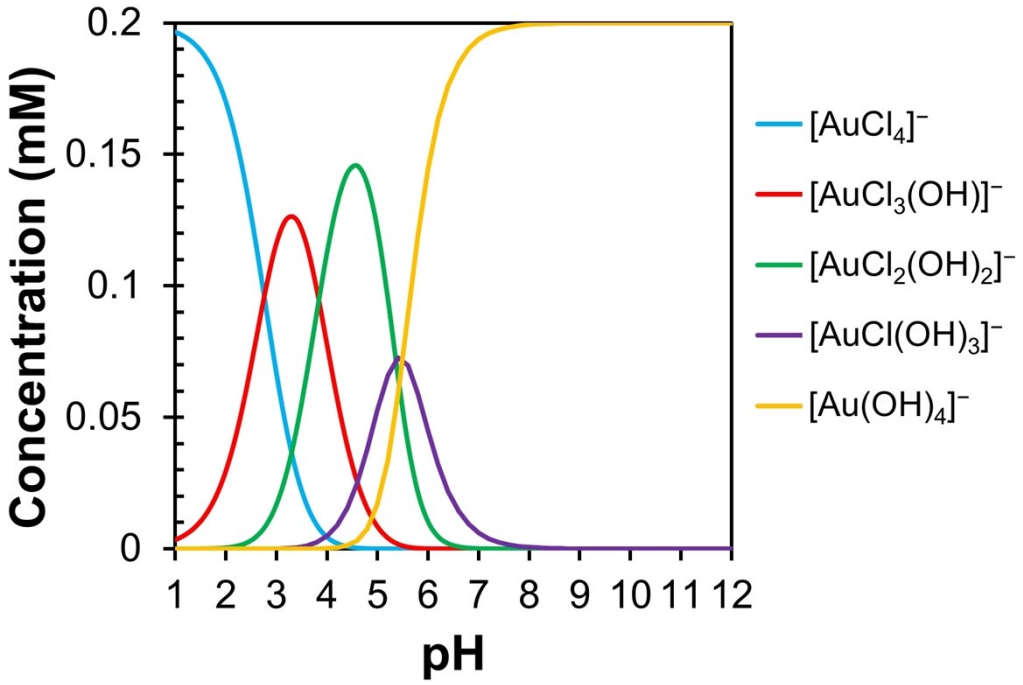

Figure S13. Calculated distribution curves of Au(III) hydroxide complexes ($[AuCl_{4-n}(OH)_n]^-$) in the presence of Cl^- (0.8 mM). Total Au concentration: 0.2 mM. Speciation was calculated based on the dissociation constants of Au(III) hydroxide complexes reported by Usher et al.[S1]

S1. A. Usher, D. C. McPhail and J. Brugger, *Geochim. Cosmochim. Acta*, 2009, **73**, 3359–3380.

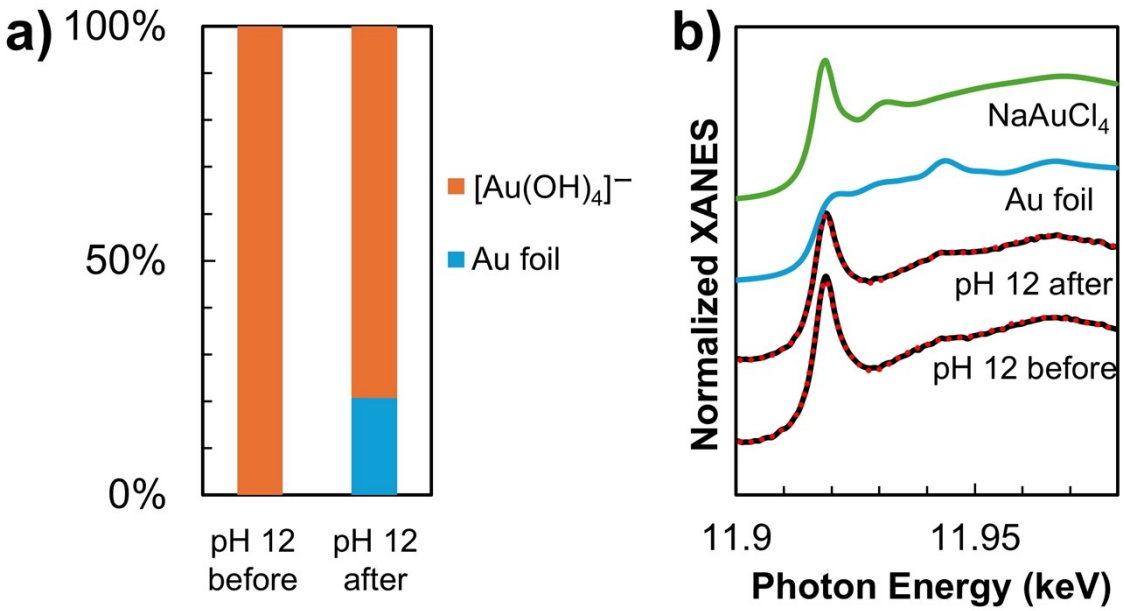

Figure S14. XANES analysis of Au complexes before and after heating at pH 12. (a) Principal component analysis (PCA) results showing the transformation of Au complexes upon heating. Only $Au(OH)_4^-$ was present before heating, and partial transformation into metallic Au was observed after heating. (b) Normalized XANES spectra of reaction solutions before and after heating: solid line, experimental data; dotted line, fit to standards. These spectra were used for PCA.

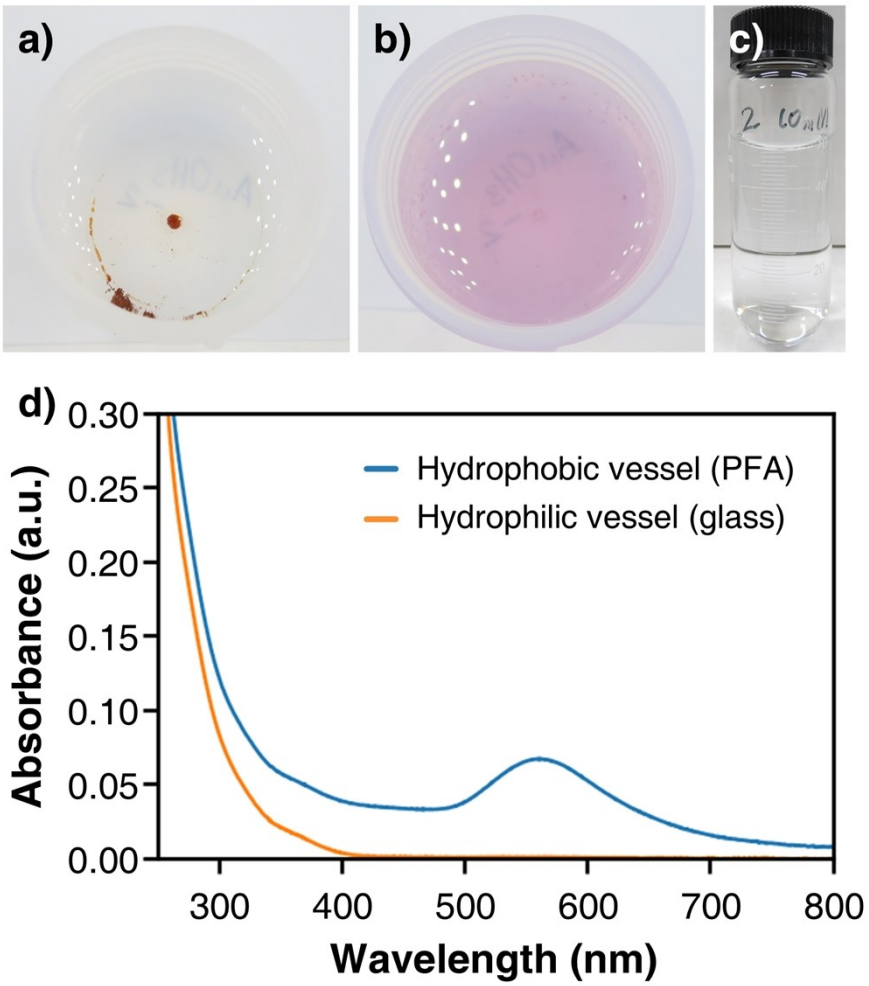

Figure S15. AuNP synthesis using $Au(OH)_3$ as a precursor. (a) Photograph of the reaction mixture before heating where undissolved $Au(OH)_3$ is visible. (b) After heating in a hydrophobic PFA vessel, the solution turned red, indicating AuNP formation. (c) After heating in a hydrophilic glass vessel, the solution remained colorless, suggesting no AuNP formation. (d) UV–vis spectra of solutions reacted in hydrophobic and hydrophilic vessels. The final pH values were 11.9 (PFA) and 12.0 (glass), indicating that both reactions proceeded under similarly alkaline conditions.

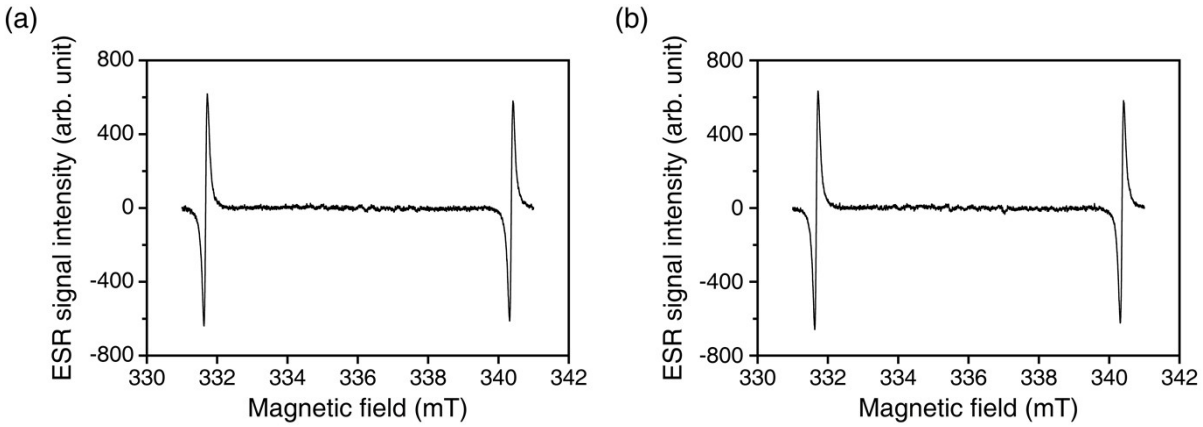

Figure S16. ESR spectra of the reaction solution containing DMPO obtained from the PFA vessel after heating at 80 °C for (a) 30 min and (b) 60 min. Only the Mn^{2+} marker signals are observed at ~331.5 and ~340.5 mT.

Electron spin resonance (ESR) analysis was performed using a JEOL JES-FA-100 spectrometer under the following conditions: field sweep, 330.9–340.9 mT; field modulation frequency, 100 kHz; field modulation width, 0.1 mT; amplitude, 100; sweep time, 2 min; time constant, 0.03 s; microwave frequency, 9.427 GHz; microwave power, 4 mW. The spin-trapping agent 5,5-dimethyl-1-pyrroline-*N*-oxide (DMPO) was added for the detection of free radicals. A Mn^{2+} marker was placed in the ESR cavity as an internal standard. An aqueous solution of $HAuCl_4$ and NaOH was heated in a hydrophobic PFA vessel and subsequently analyzed by ESR.

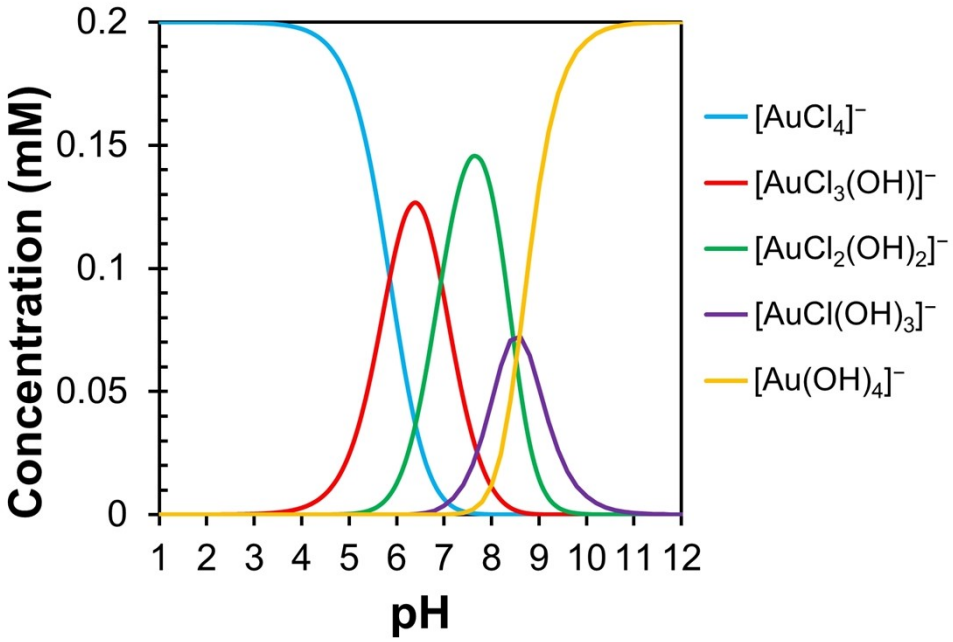

Figure S17. Calculated distribution curves of Au(III) hydroxide complexes ($[AuCl_{4-n}(OH)_n]^-$) in the presence of Cl^- (≈ 1 M) introduced by addition of 1 M NaCl. Total Au concentration: 0.2 mM.

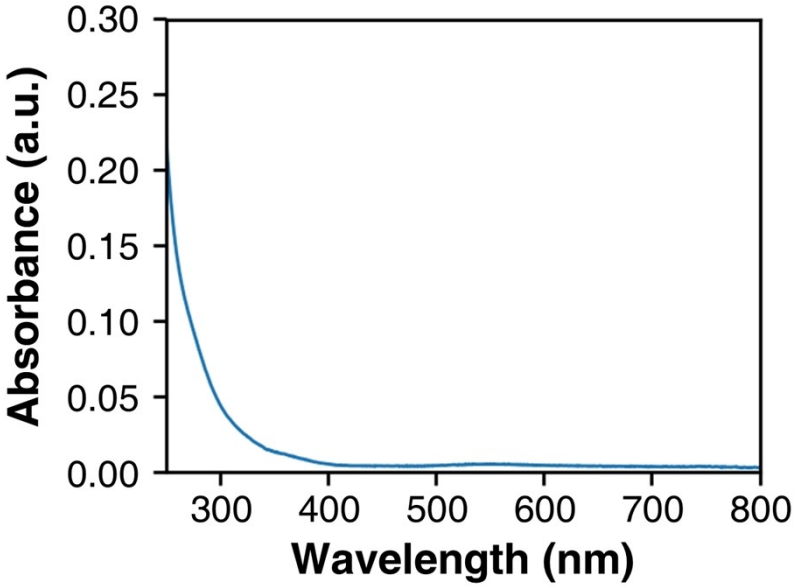

Figure S18. UV–vis spectrum of the product obtained under standard conditions (pH 12, 80 °C, 20 h, PFA vessel) with the addition of 1 M NaCl solution.

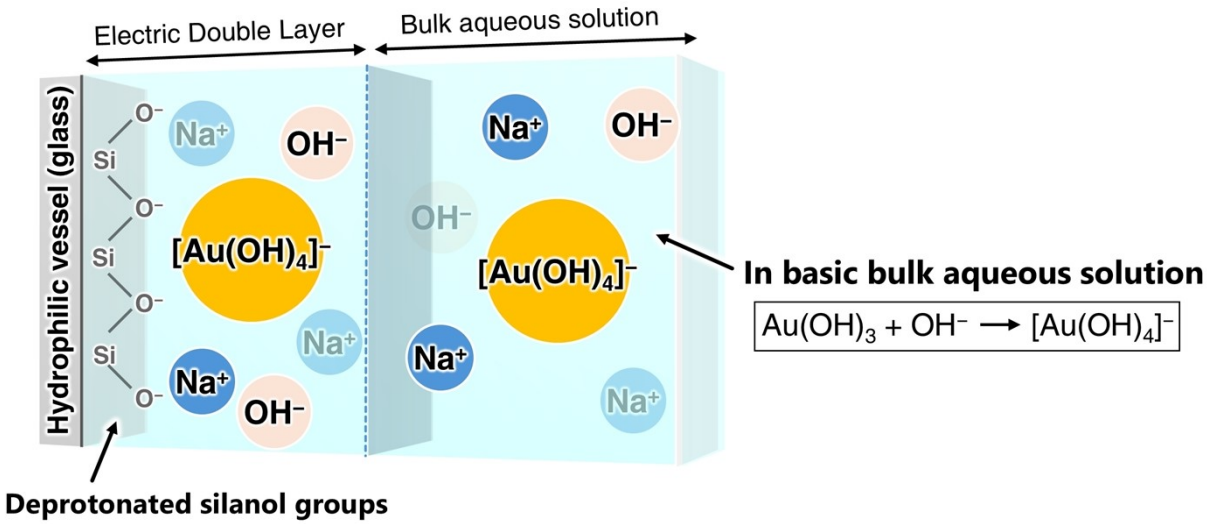

Figure S19. Schematic of a possible mechanism for the suppression of AuNP formation at hydrophilic interfaces under basic conditions. Deprotonated silanol groups generate a negatively charged interfacial region at the glass/water interface. As a result, near-interface ion partitioning is expected to differ fundamentally from that at PFA/water interfaces and is unlikely to support the specific local OH^- depletion proposed to promote $Au(OH)_3$-like nucleation. Consequently, the interfacial formation of $Au(OH)_3$-like species, and thus reductant-free AuNP formation, is suppressed.

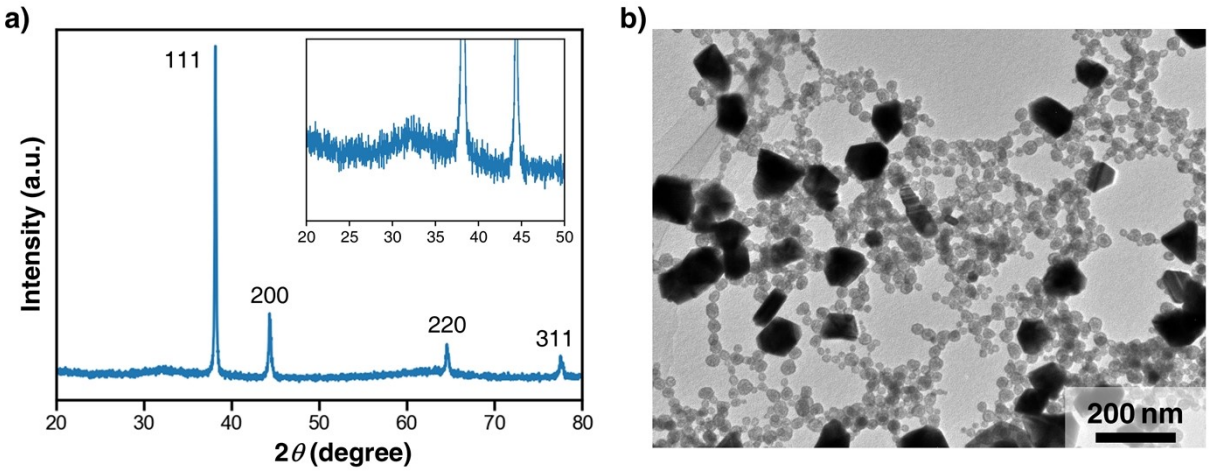

Figure S20. (a) XRD pattern and (b) TEM image of the product obtained by hydrothermal treatment of colloidal $Au(OH)_3$ at 140 °C for 10 h. Colloidal $Au(OH)_3$ was prepared in a PFA vessel under Category II (weakly acidic) conditions at 80 °C for 20 h, then transferred to a PTFE-lined autoclave and subjected to hydrothermal treatment at 140 °C for 10 h. Diffraction peaks assignable to metallic Au are observed alongside a broad pattern of amorphous $Au(OH)_3$. The TEM image shows irregularly shaped AuNPs coexisting with unreacted spherical $Au(OH)_3$ particles, confirming partial thermolysis under these conditions.

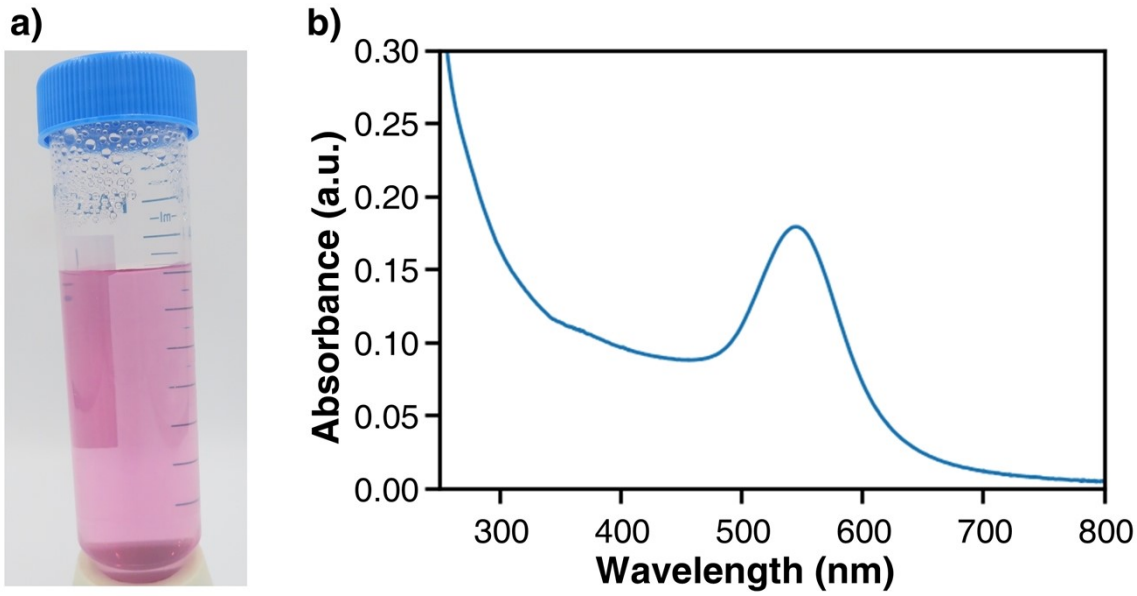

Figure S21. AuNP synthesis in a polypropylene (PP) vessel. (a) Photograph and (b) UV–vis spectrum of the reaction solution.

Table S1. pH values of reaction solutions before and after heating under different conditions. Measured pH values (before/after heating) for each category (I–III) in hydrophobic PFA and hydrophilic glass vessels. The observed pH decrease in Category II is attributed to proton generation during the hydrolysis of $[AuCl_{4-n}(OH)_n]^-$ ($1 \leq n \leq 3$) to form $Au(OH)_3$.

			Hydrophobic vessel (PFA)		Hydrophilic vessel (glass)	
			Before	After	Before	After
Category I	HCl	100 mM	1.2	1.2	1.1	1.1
Category II	NaOH	0 mM	3.3	3.2	3.5	3.3
	NaOH	1 mM	5.7	4.4	6.9	5.2
Category III	NaOH	2 mM	10.5	10.3	10.5	10.2
	NaOH	5 mM	11.5	11.6	–	–
	NaOH	10 mM	11.9	11.9	12.0	11.9

Table S2. AuNP synthesis conditions using hydrophobic PFA vessels and indicators obtained from UV–vis spectra. For each condition, indicator values are the averages of at least two independent repetitions.

$HAuCl_4$ (mM)	NaOH (mM)	Temperature (°C)	Time (h)	λ_{spr}	A_{spr}/A_{450}	A_{400}
Influence of solution pH						
1	2	80	20	555	2.04	0.03
	5			552	1.99	0.06
	10			540	1.88	0.09
	50			540	1.26	0.01
Influence of reaction temperature						
1	10	25	14 days	528	1.44	0.01
		60		530	1.72	0.01
		80	20	540	1.88	0.09
		100		548	1.93	0.12
Influence of reaction time						
1	10	80	5	539	1.80	0.02
			10	537	1.80	0.03
			20	540	1.88	0.09
			40	548	1.91	0.11
			60	542	1.90	0.13
			70	537	1.86	0.11
			80	541	1.89	0.13
Influence of initial $HAuCl_4$ concentration						
0.2	10	80	20	549	1.93	0.03
1				540	1.88	0.09
3				531	1.65	0.08
5				532	1.64	0.09

Table S3. Zeta potential at pH ≈ 10 on hydrophobic PFA and hydrophilic glass substrates.

Hydrophobic PFA substrate		Hydrophilic glass substrate	
pH	Zeta potential (mV)	pH	Zeta potential (mV)
10.04	−85.81	10.06	−70.98
10.05	−77.14	10.06	−70.22
10.03	−87.24	10.04	−73.04
Average	−83.4±4.2	Average	−71.4±1.1

Zeta potential measurements of the PFA and glass substrates were performed using the streaming-potential method (SurPASS3, Anton Paar). A 1 mM KCl solution was used as the reference electrolyte, and the pH was adjusted by incremental additions of KOH. The substrates were mounted in the cell, and the streaming potential was recorded while varying the pressure; the zeta potential was calculated according to the Helmholtz–Smoluchowski equation.

Estimation of Debye length (λ_D)

The Debye length (λ_D) for an electrolyte solution is given by the linearized Poisson–Boltzmann (Debye–Hückel) expression:

$$\lambda_D = \sqrt{\frac{\varepsilon_0 \varepsilon_r k_B T}{2 N_A e^2 I}}$$

where ε_0 is the vacuum permittivity (8.854×10^{-12} F/m), ε_r is the relative permittivity of water (≈ 78.5 at 25 °C), k_B is the Boltzmann constant (1.381×10^{-23} J/K), T is the absolute temperature (≈ 298 K), N_A is Avogadro's number (6.022×10^{23} mol^{-1}), e is the elementary charge (1.602×10^{-19} C), and I is the ionic strength (mol/L). For aqueous solution at 25 °C, this simplifies to the widely used approximation:

$$\lambda_D \approx \frac{0.304}{\sqrt{I}} \text{ (nm)}$$

Mixtures were prepared by combining 10 mL of 1 mM $HAuCl_4$ with 40 mL of NaOH at the specified stock concentrations (final volume 50 mL). Thus, $C_{[NaOH,final]} = 0.8 \cdot C_{[stock]}$. Total Au(III) after mixing is 0.2 mM. At high pH, bulk Au(III) is dominated by $[Au(OH)_4]^-$. During ligand exchange from $[AuCl_4]^-$ to $[Au(OH)_4]^-$, four equivalents of Cl^- are released and four equivalents of OH^- are consumed per Au(III) center; in addition, one equivalent of OH^- is consumed to neutralize H^+ from $HAuCl_4$. Hence, for [Au] = 0.2 mM, $\Delta[Cl^-] = +0.8$ mM and $\Delta[OH^-] = -1.0$ mM. Under these assumptions, for cases (1)–(5) without added NaCl, $I = C_{[NaOH,final]}$ exactly. Case (6) adds NaCl to achieve 1.0 M NaCl in the final mixture; the volume change upon NaCl addition is neglected in estimating I.

Results (25 °C)

Table S4. Debye lengths (λ_D) estimated from solution ionic strength

Case	pH (exp.)	$HAuCl_4$ stock (mM)	$HAuCl_4$ vol. (mL)	NaOH stock (mM)	NaOH vol. (mL)	NaCl final (M)	NaOH final (M)	I (M)	λ_D (nm)
(1)	10.3	1	10	2	40	–	0.0016	0.0016	7.600
(2)	11.6	1	10	5	40	–	0.004	0.004	4.807
(3)	11.9	1	10	10	40	–	0.008	0.008	3.399
(4)	12.7	1	10	50	40	–	0.04	0.04	1.520
(5)	13.7	1	10	1000	40	–	0.8	0.8	0.340
(6)	–	1	10	10	40	1	0.008	1.008	0.303

Notes

- The 25 °C approximation applies to aqueous solutions only; for other temperatures or solvents, use the general expression with $\varepsilon_r(T)$ and T.
- Ionic strength was evaluated for monovalent species {Na^+, OH^-, Cl^-, $[Au(OH)_4]^-$}; activity effects and minor mixed chloro–hydroxo species are neglected in the present calculation.
- In case (6), $I \approx 1.008$ M and $\lambda_D \approx 0.303$ nm, owing to the dominance of 1.0 M NaCl.